Electronic Supplementary Information for:

Direct O_2 mediated oxidation of a Ni(II)-N_3O structural model for the active site of nickel acireductone dioxygenase (Ni-ARD): Characterization, biomimetic reactivity, and enzymatic implications

Kelsey, E. Kirsch;[a] Mary E. Little;[b] Thomas R. Cundari;[c] Emily El-Shaer;[b] Georgia Barone;[b] Vincent M. Lynch;[d] Santiago A. Toledo[a]

a. Department of Chemistry, American University, 4400 Massachusetts Ave NW, Washington, DC, 20016, United States of America.
b. Department of Chemistry, St. Edward's University, 3001 South Congress Ave, Austin, Texas 78704, United States of America.
c. Department of Chemistry, University of North Texas, 1155 Union Cir, Denton, Texas 76203, United Sates of America
d. Department of Chemistry, The University of Texas at Austin, 120 Inner Campus Dr Stop G2500, Austin, Texas 78712, United States of America.

Supporting information table of contents	**page**
Characterization of ligand L1	**4-5**
Figure S1. ^{1}H NMR (300 MHz, $CDCl_3$) of L1	4
Figure S2. ^{13}C NMR (300 MHz, $CDCl_3$) of L1	5
Figure S3. UV-Visible spectrum of L**1** in CH_3OH	5
Characterization of complex 1	**6-11**
Figure S4. UV-Visible spectrum of **1** in CH_3OH	6
Figure S5. ^{1}H NMR spectrum of complex **1** in CD_3OD.	7
Figure S6. Cyclic voltammogram of complex **1** in MeCN	8
Figure S7. Cyclic voltammogram of the titration of complex **1** in MeCN and addition of 2HAP-H and Et_3N	9
Figure S8. Cyclic voltammogram of Fe-N3O analogue of **1** in MeCN	10
Image S1. HR-ESI-MS of **1**	10
Image S2. Elemental analysis results for **1** (C, H, N only)	11
Additional complexes	**12**
Figure S9. UV-Visible spectrum of **1**-acac (**2**) in CH_3OH	12

Characterization of ligand L1

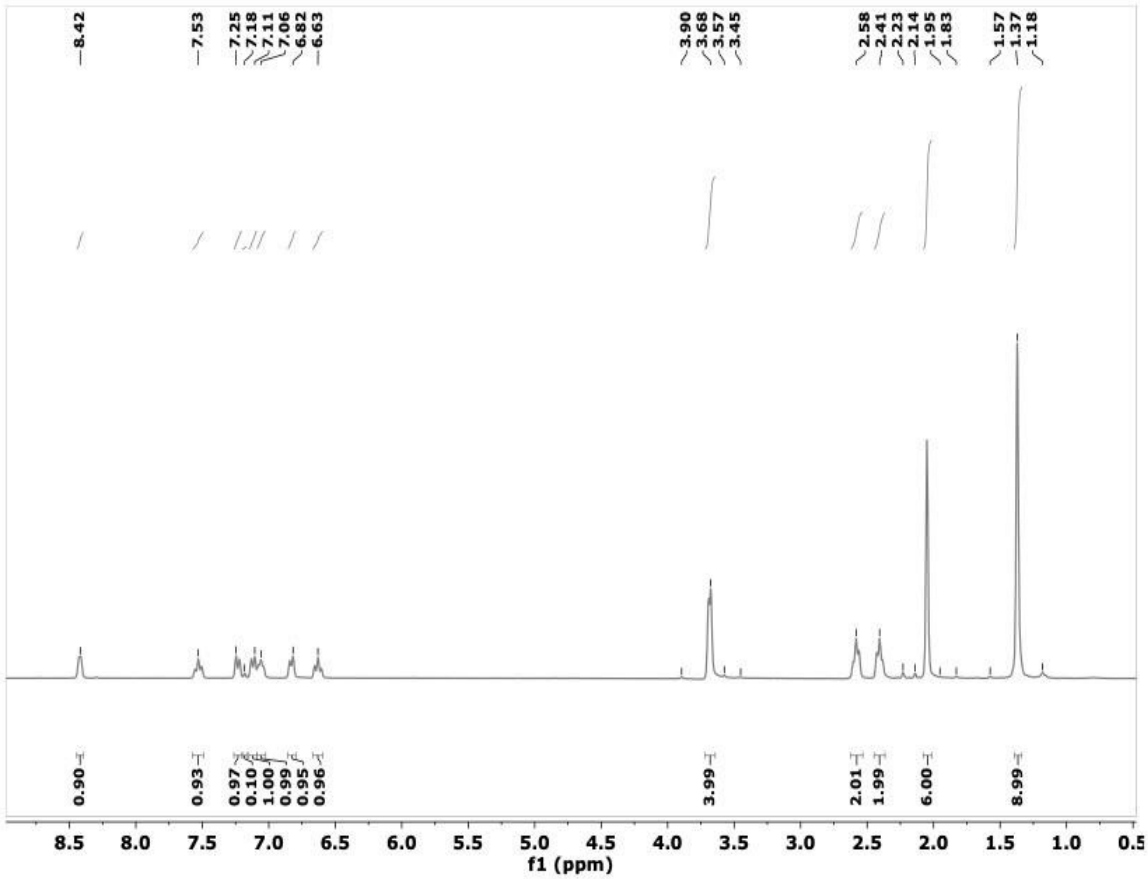

Figure S1. ^{1}H NMR (300.1 MHz, $CDCl_3$, 298 K) of L1 δ8.42 (d, 1H), 7.53 (t, 1H), 7.25 (d, 1H), 7.11 (t, 1H), 7.06 (d, 1H), 6.82 (d, 1H), 6.63 (t, 1H), 3.68 (s, 4H), 2.58 (t, 2H), 2.41 (t, 2H), 1.95(s, 6H), 1.37 (s, 9H).

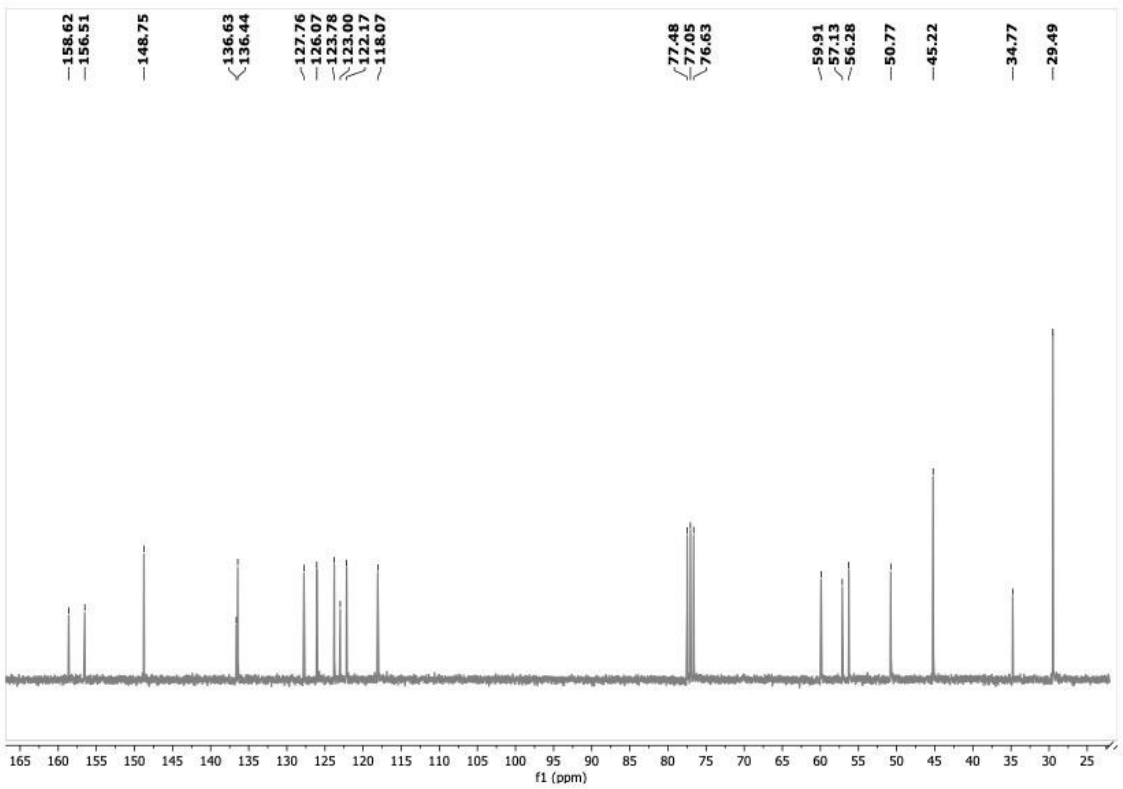

Figure S2. ^{13}C NMR (300.1 MHz, $CDCl_3$, 298 K) of **L1**

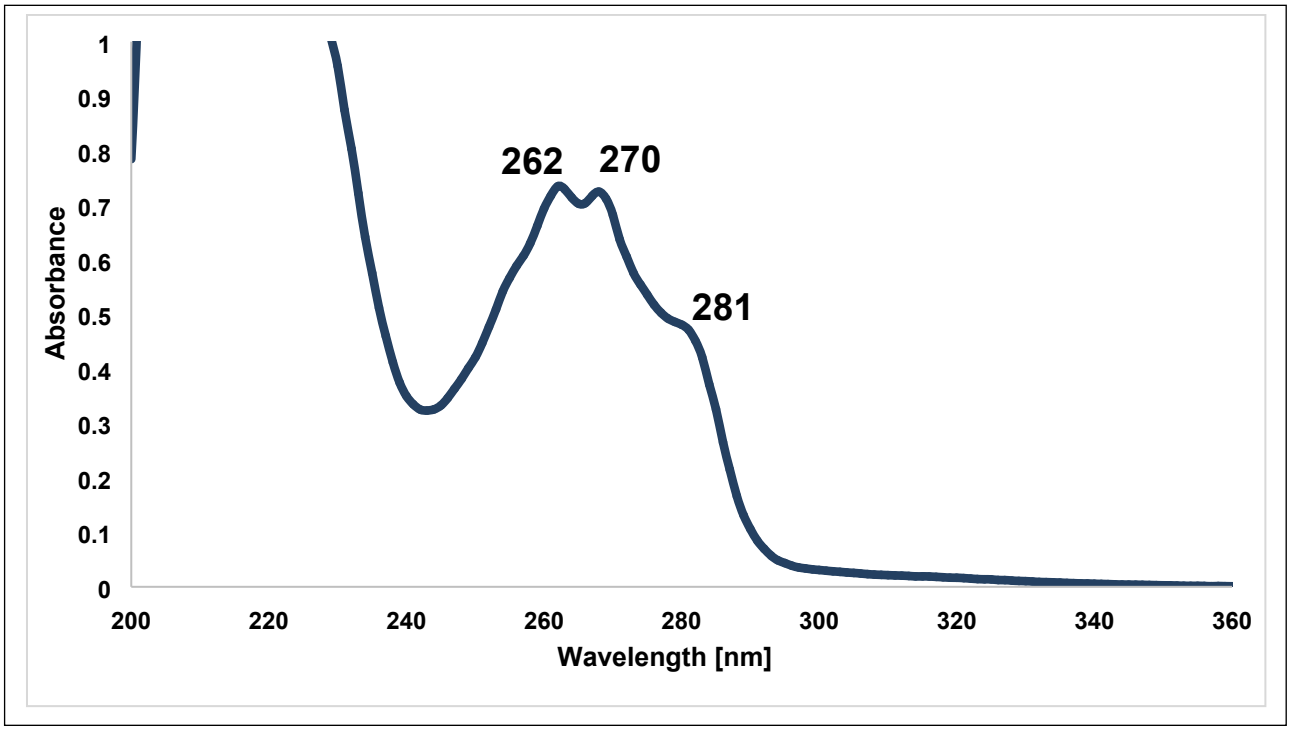

Figure S3. UV-Visible spectrum of **L1** in CH_3OH.

Characterization of complex 1

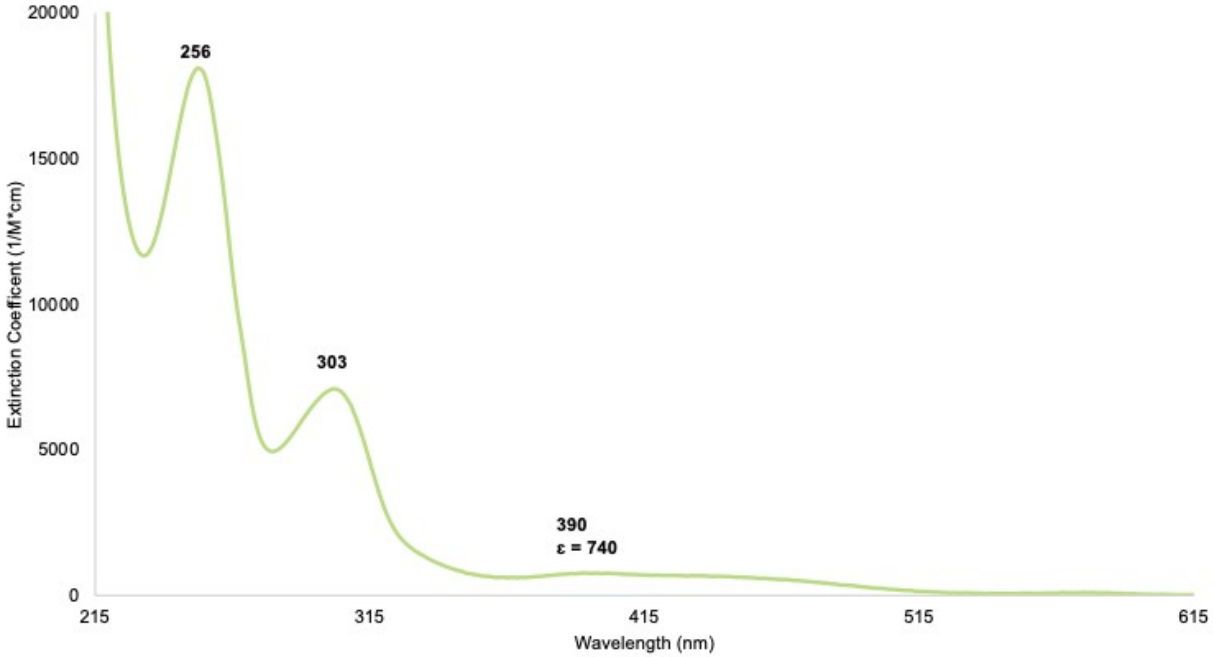

Figure S4. UV-Visible spectrum of **1** in CH_3OH

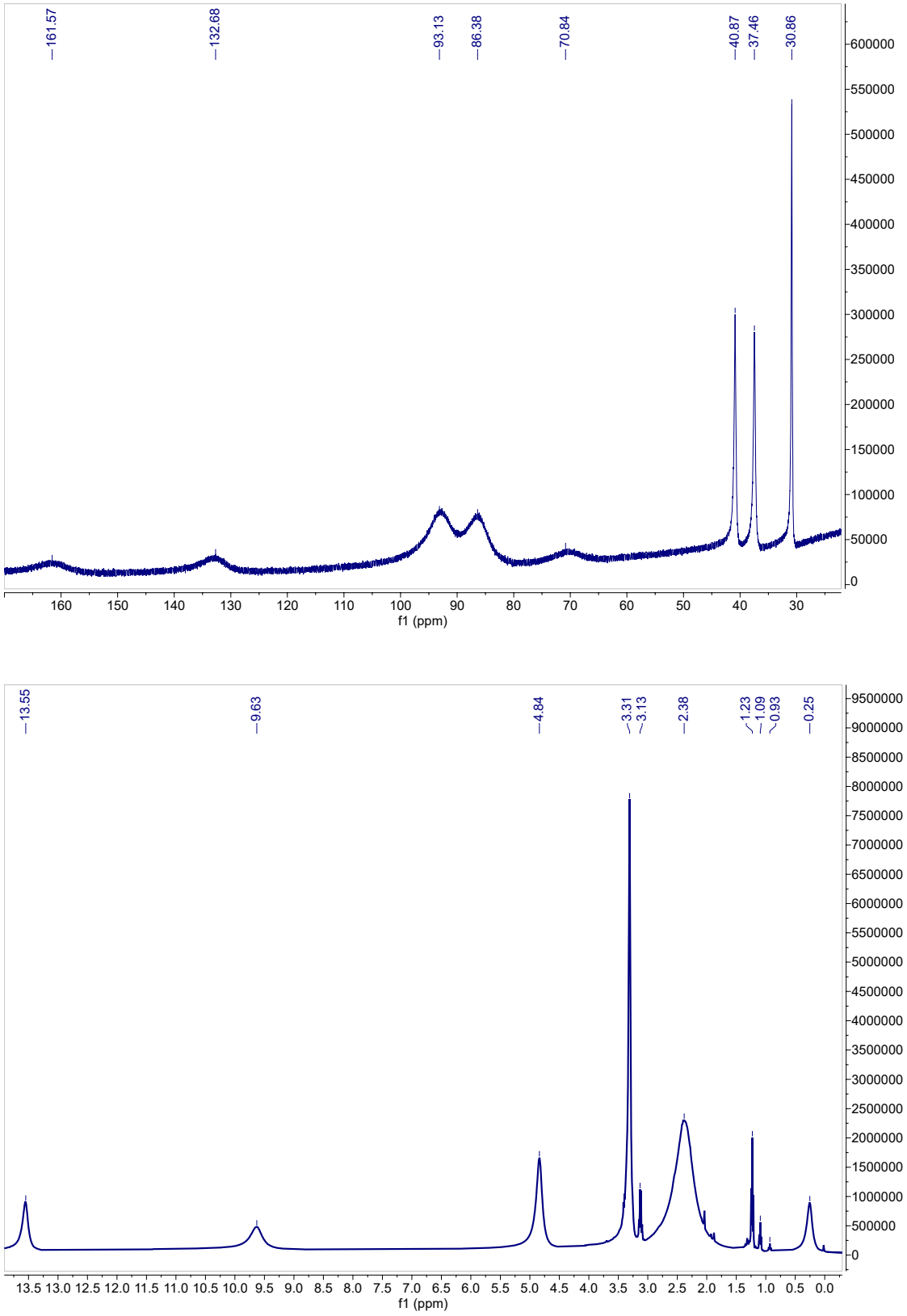

Figure S5. ^{1}H NMR spectrum of **1** (400.1 MHz, CD_3OD, 298 K).

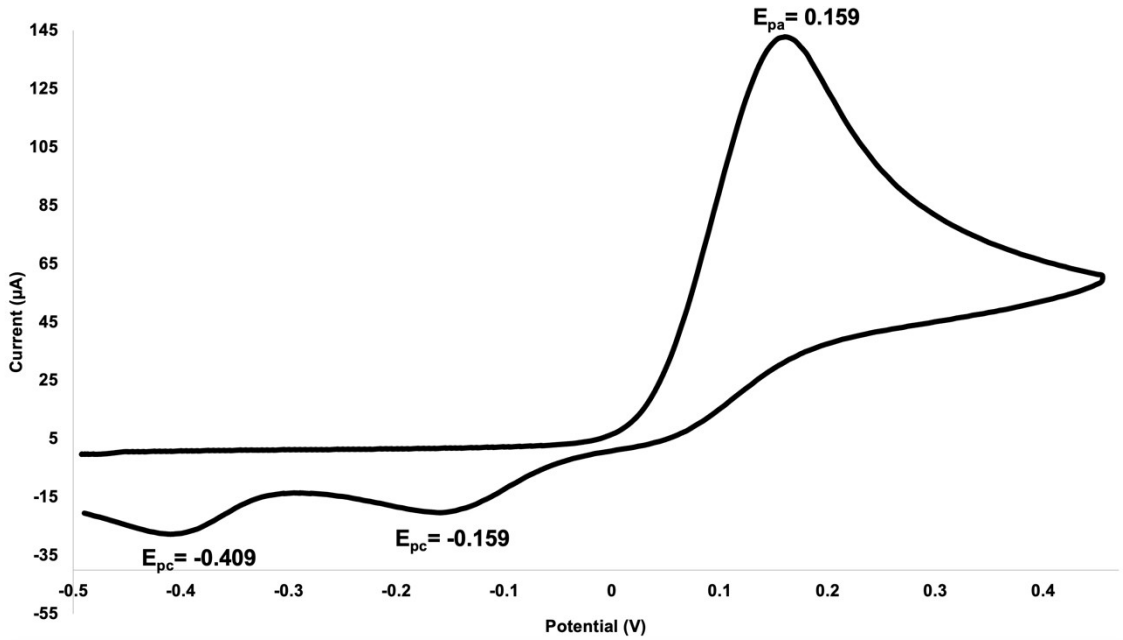

Figure S6. Cyclic voltammogram of **1** in MeCN (2.72mM) containing $[NBu_4][PF_6]$ (0.1M) as the supporting electrolyte. Scan rate 250 mV/sec. Potentials reported vs. Fc/Fc^+**.**

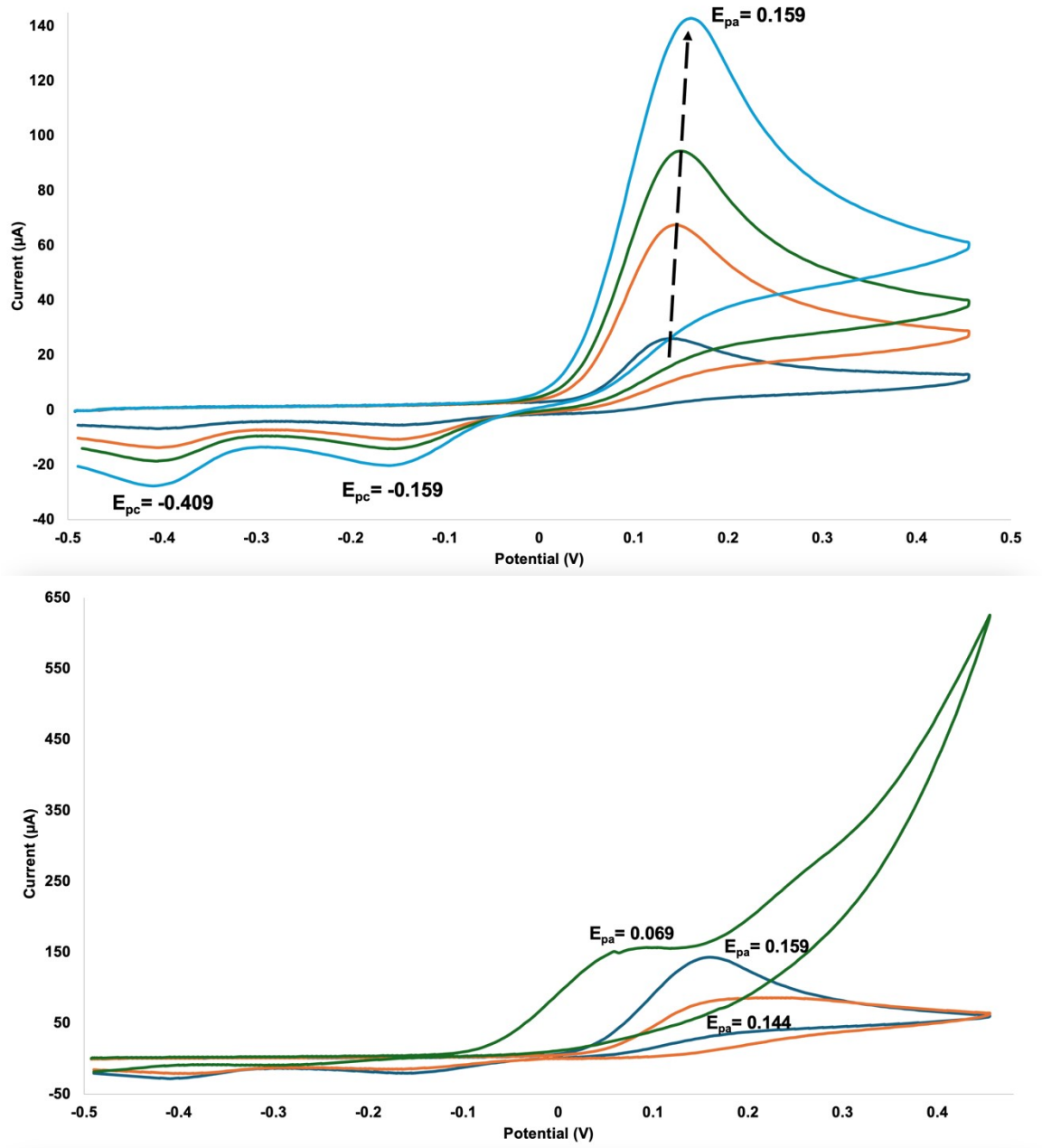

Figure S7. Top: Cyclic voltammogram of the titration of complex **1** in MeCN (growth after addition of 0.25 eq. to 1eq.) (1.11 mM final concentration of **1**) Bottom: complex **1** (blue trace) with addition of 20 eq. of 2HAP-H (orange trace) and 1 eq. of Et_3N (green trace-anodic shift) containing $[NBu_4][PF_6]$ (0.1M) as the supporting electrolyte. Scan rate 250 mV/sec. Potentials reported vs. Fc/Fc^+**.**

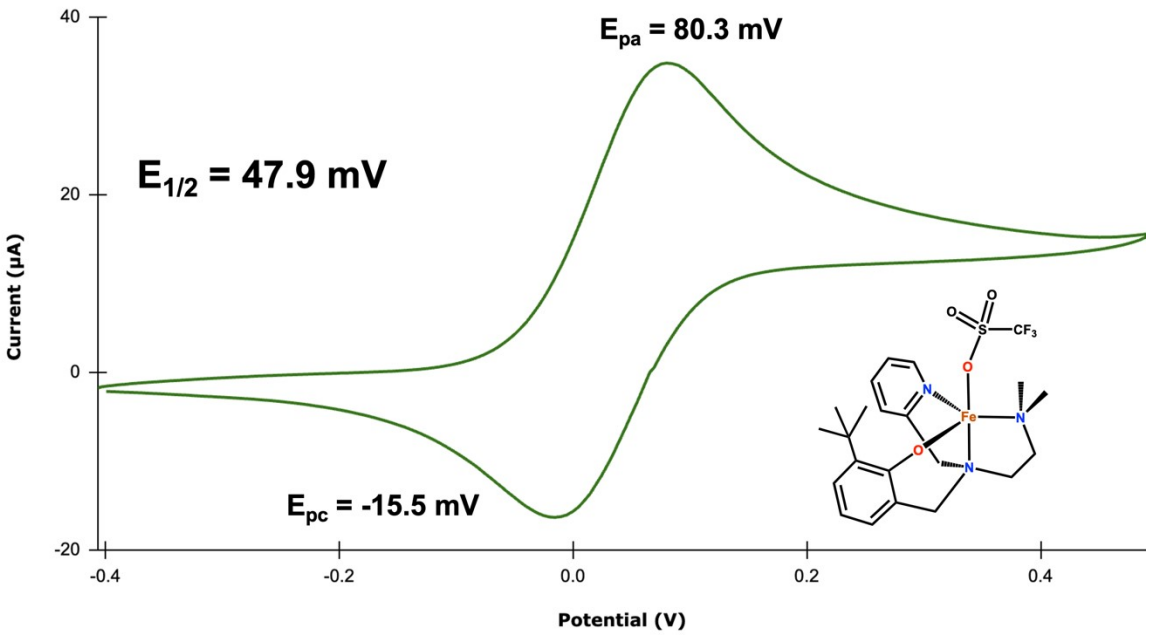

Figure S8. Cyclic voltammogram of Fe-N_3O analogue of **1** (shown in inset) in MeCN (1.5mM) containing $[NBu_4][PF_6]$ (0.1M) as the supporting electrolyte. Scan rate 250 mV/sec. Potentials reported vs. Fc/Fc^+.

Target Compound Screening Report

Results Acquired by The University of Texas at Austin Mass Spectrometry Facility

Data File	MSF20-922NiEE_hrESIpos2.d	**Sample Name**	922NiEE	**Comment**	922NiEE
Position	P1-C4	**Instrument Name**	Instrument 1	**User Name**	
Acq Method	FIA_pos.m	**Acquired Time**	9/23/2020 10:53:52 AM	**DA Method**	KS.m

MS Zoomed Spectrum

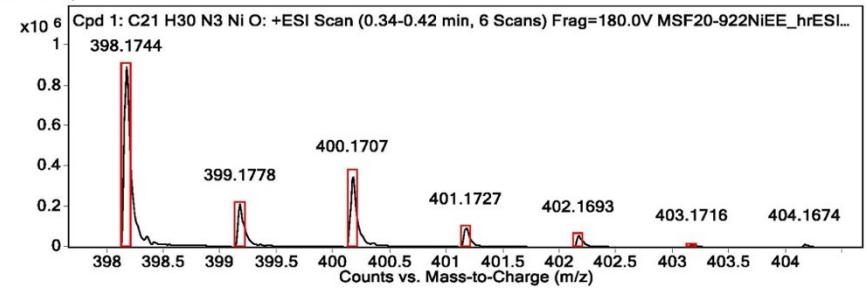

MS Spectrum Peak List

Obs. m/z	Calc. m/z	Charge	Abundance	Formula	Ion Species	Tgt Mass Error (ppm)
398.1744	398.1737	1	910252	C21H30N3NiO	M+	-1.86
399.1778	399.1768	1	214373	C21H30N3NiO	M+	-2.4
400.1707	400.1699	1	357350	C21H30N3NiO	M+	-2.02
401.1727	401.1721	1	96632	C21H30N3NiO	M+	-1.67
402.1693	402.1685	1	57260	C21H30N3NiO	M+	-1.95
403.1716	403.1706	1	13669	C21H30N3NiO	M+	-2.63
404.1674	404.1671	1	13682	C21H30N3NiO	M+	-0.9

--- End Of Report ---

Image S1. HR-ESI-MS of **1**

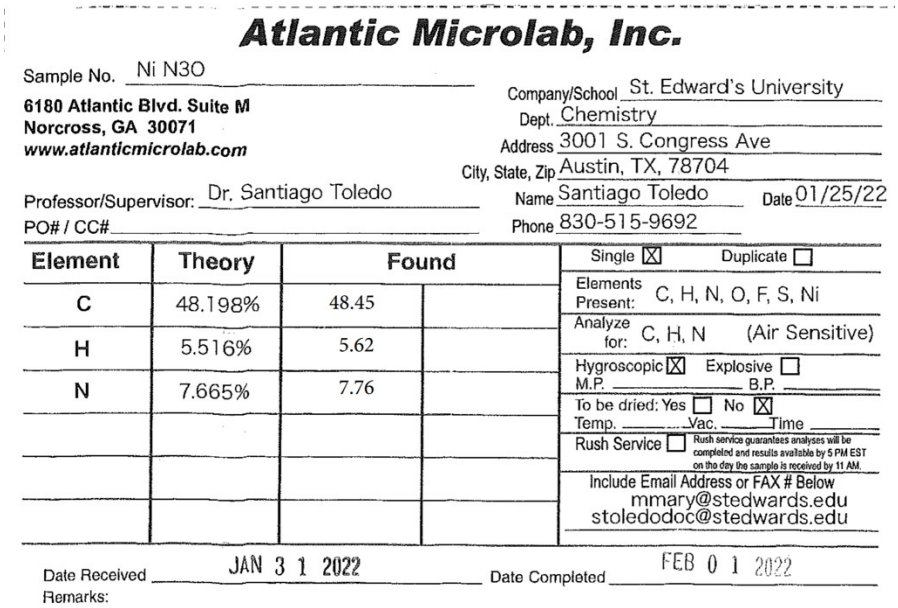

Atlantic Microlab, Inc.

Sample No. Ni N3O

6180 Atlantic Blvd. Suite M
Norcross, GA 30071
www.atlanticmicrolab.com

Company/School St. Edward's University
Dept. Chemistry
Address 3001 S. Congress Ave
City, State, Zip Austin, TX, 78704
Name Santiago Toledo Date 01/25/22
Phone 830-515-9692

Professor/Supervisor: Dr. Santiago Toledo
PO# / CC#

Element	Theory	Found	
C	48.198%	48.45	
H	5.516%	5.62	
N	7.665%	7.76	

Single ☒ Duplicate ☐
Elements Present: C, H, N, O, F, S, Ni
Analyze for: C, H, N (Air Sensitive)
Hygroscopic ☒ Explosive ☐
M.P. B.P.
To be dried: Yes ☐ No ☒
Temp. Vac. Time
Rush Service ☐ Rush service guarantees analyses will be completed and results available by 5 PM EST on the day the sample is received by 11 AM.
Include Email Address or FAX # Below
mmary@stedwards.edu
stoledodoc@stedwards.edu

Date Received JAN 3 1 2022 Date Completed FEB 0 1 2022
Remarks:

Image S2. Elemental analysis results for **1** (C, H, N only)

Additional complexes

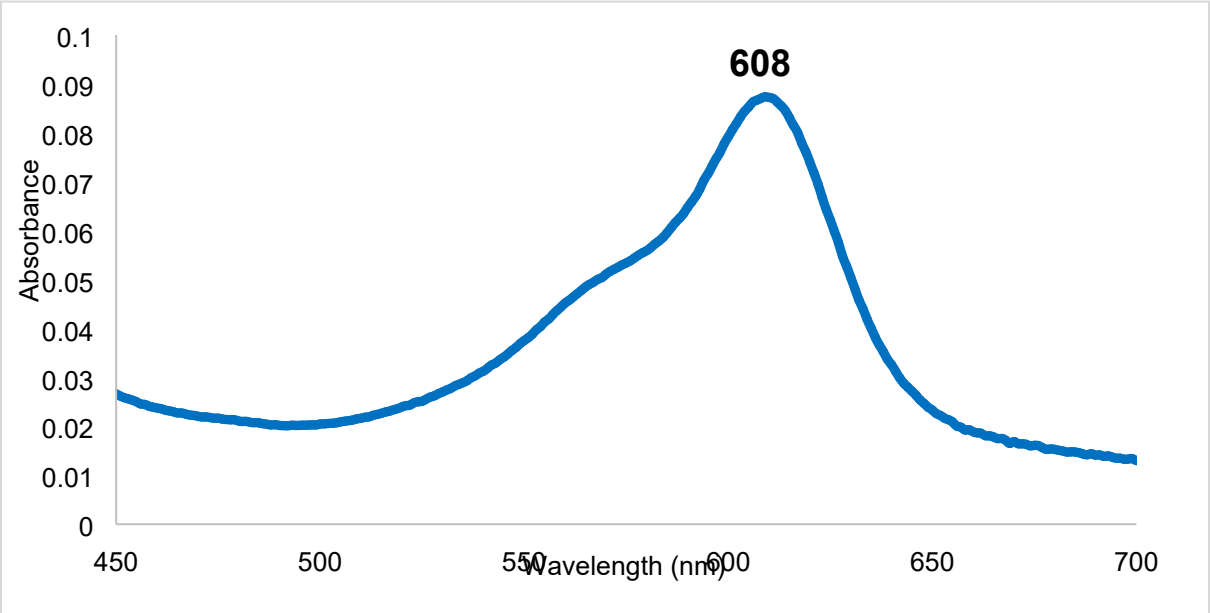

Figure S9. UV-Visible spectrum of **1-acac (2)** in CH_3OH

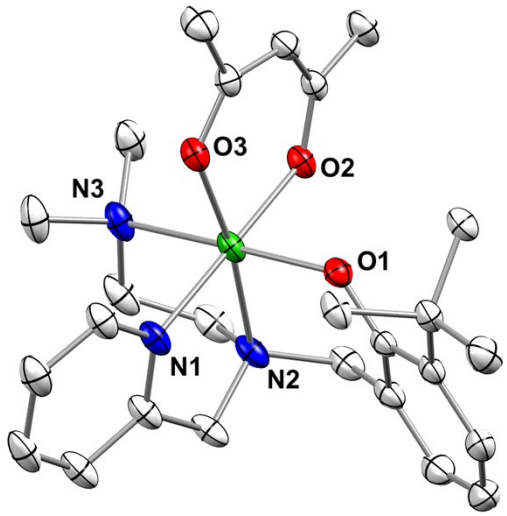

Figure S10. ORTEP representation of **1-acac** (**2**) with ellipsoids drawn at the 50% probability level. H atoms and counterions are omitted for clarity.

Synthesis of 1-acac (**2**): Complex **2** was synthesized from the addition of 5 eq. of lithium acetylacetonate to a methanolic solution of **1**. The mixture was allowed to stir for 24 hrs. and the resulting white precipitate was filtered out. The volatiles were evaporated under reduced pressure and the resulting pale blue powder was washed 3x with diethyl ether. Note the complex has marginal solubility in this solvent. The resulting powder was isolated via filtration and set up for slow vapor diffusion of diethyl ether into a 2-butanone solution of the powder. After 48 hrs. pale blue crystals of **2** were obtained.

Biomimetic oxidative C-C bond cleaving reactivity

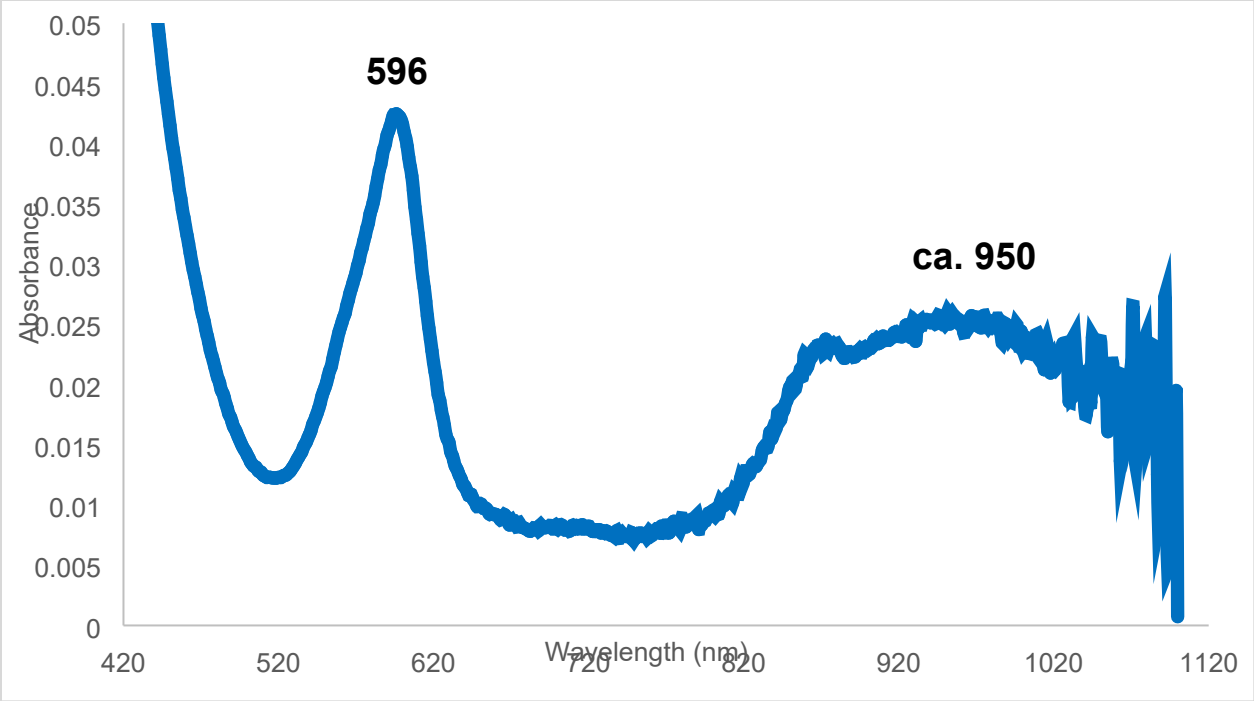

Figure S11. UV-Visible spectrum of **1**-2HAP in CH_3OH

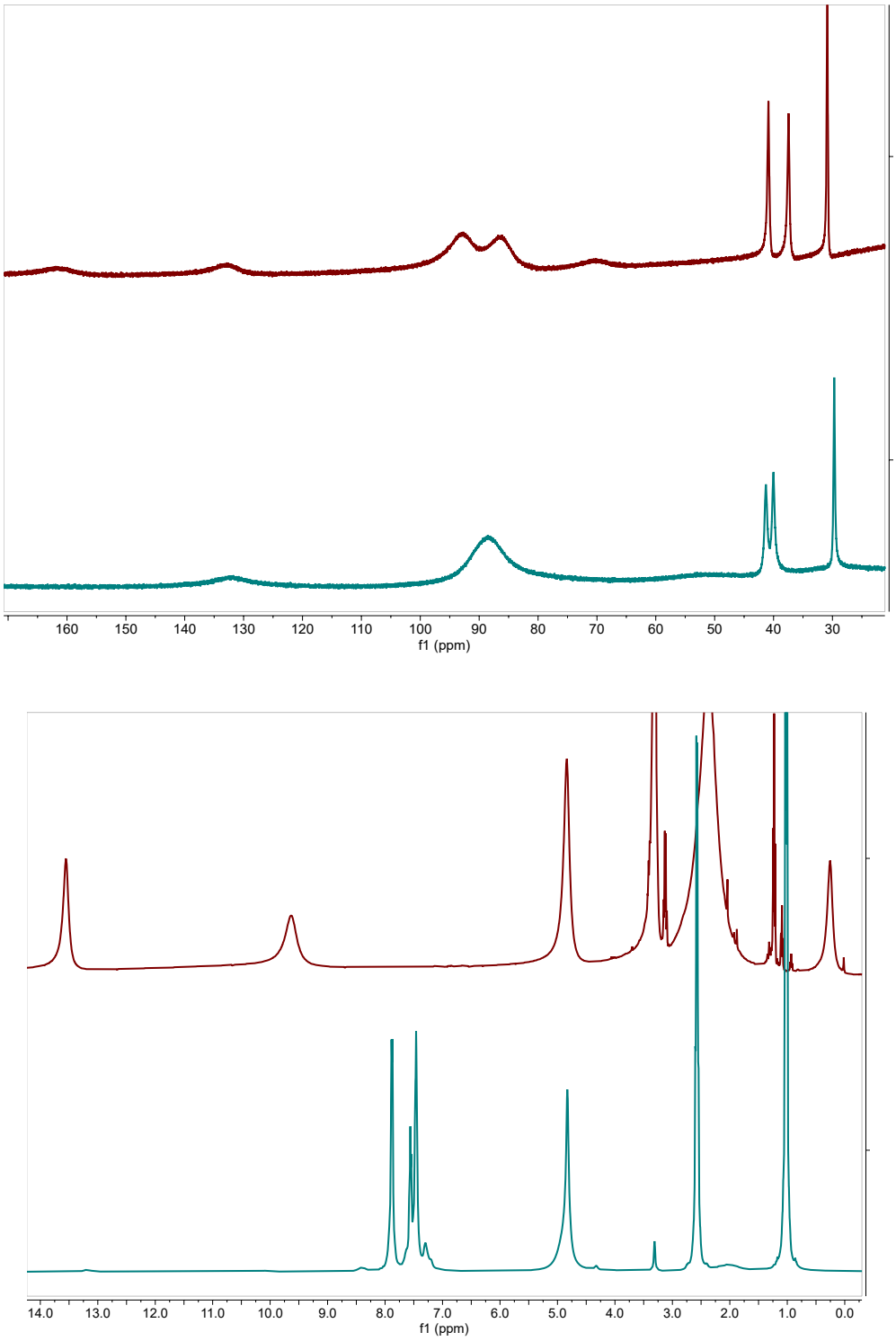

Figure S12. ^{1}H NMR **(**400.1 MHz, CD_3OD, 298 K**)** spectrum of **1** (red trace) compared to **1** with 20 eq. of 2HAP-H + 2eq of Et_3N (proposed **1-2HAP)** (teal trace**)**. Note the significant differences upon binding of substrate to **1**.

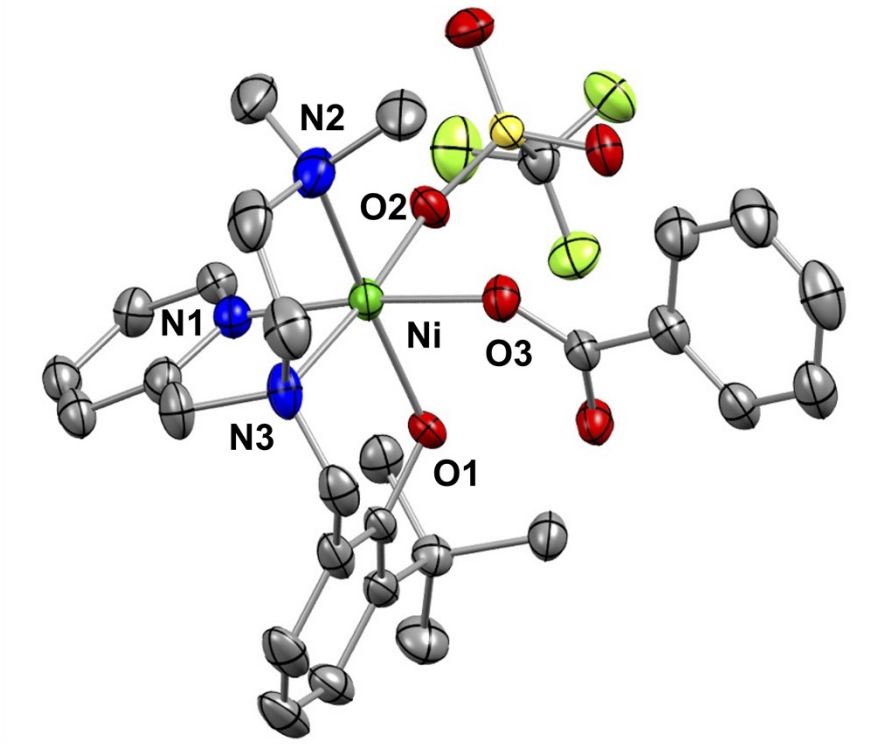

Figure S13. ORTEP representation of **1**-Benzoic acid (**3**) with ellipsoids drawn at the 50% probability level. H atoms and counterions are omitted for clarity.

Synthesis of 1-Benzoic acid (**3**): During our attempts to crystallize **1**-2HAP, complex **3** resulted from slow evaporation of dichloromethane solutions of a blue/green powder that resulted from the reaction of **1** with 20 eq. of 2HAP-H and 2 eq. Et_3N in MeCN. The resulting mixture was dried under vacuum and the crude material triturated with diethyl ether 3x. The resulting bluish powder was dissolved in minimum dichloromethane and placed in a vial with a small gauge needle. Over the course of three days, pale yellow crystals resulted. The bulk of the material was analyzed through various samples and consistently yielded the complex shown in figure S16SX (**1**-Benzoic acid). This we presume resulted from the oxidative cleavage of 2HAP by **1**, in the presence of trace adventitious O_2 in the solvent mixture.

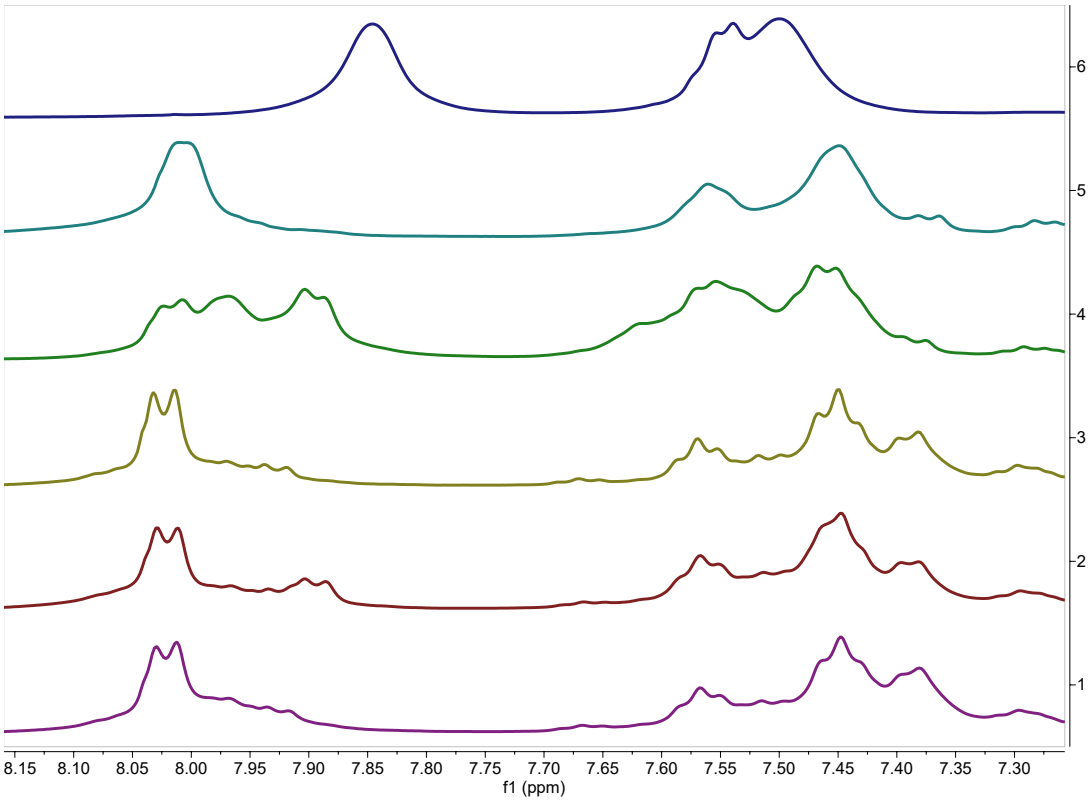

Figure S14. ^{1}H-NMR in CD_3OD of the reaction mixture between **1**, 1 eq. of 2HAP-H, 2 eq. of Et_3N, under N_2 (blue trace). Reaction mixture after addition of 60 minutes of O_2 (teal trace). Note the complete disappearance of starting material 2HAP-H. Addition of 2 additional eq. 2HAP-H (3 eq total, green trace), addition of 80 more minutes of O_2 (yellow trace), addition of 2 more eq 2HAP-H (5 eq total, brown trace), and 80 more minutes of O_2 (purple trace).

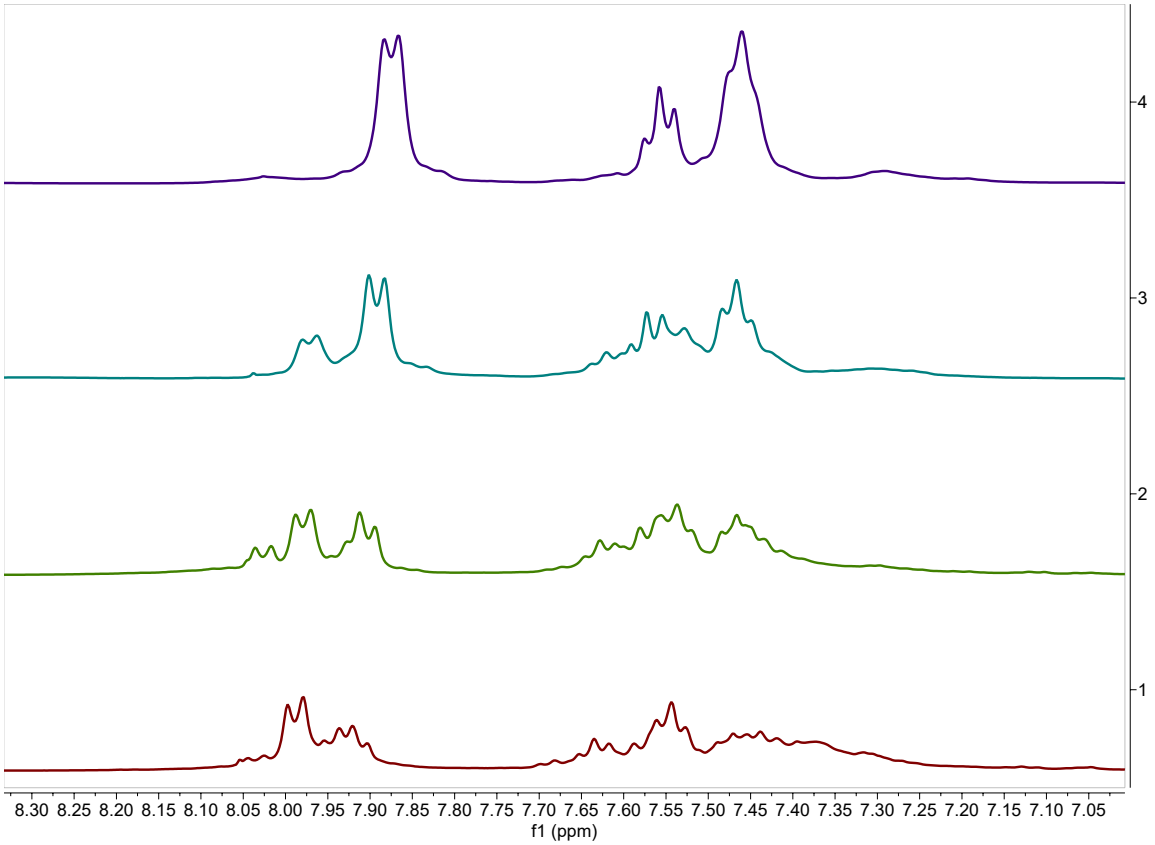

Figure S15. ^{1}H-NMR in CD_3OD of the reaction mixture between **1,** 20 eq of 2HAPH, 2 eq of triethyl amine (Et_3N) under N_2 (purple trace). Reaction mixture after addition of 40 minutes of O_2 (teal trace). Addition of 40 more minutes of O_2 (green trace), and 20 more minutes of O_2 and 20 hours of reaction time (brown trace-bottom).

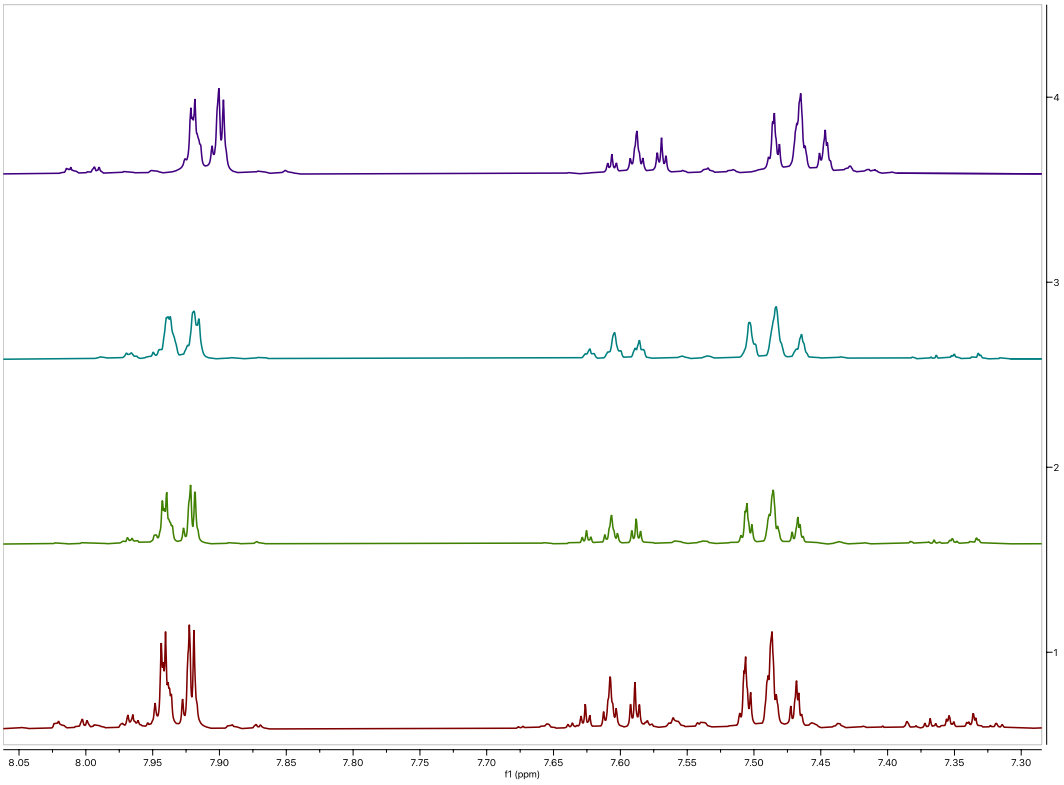

Figure S16. ^{1}H-NMR in CD_3OD of the reaction mixture between 20 eq of 2HAPH, under N_2 (purple trace). Reaction mixture after addition of 2 eq of triethyl amine (Et_3N) (teal trace). Reaction mixture after addition of 40 minutes of O_2 (green trace), and 2 hours of reaction time (brown trace-bottom).

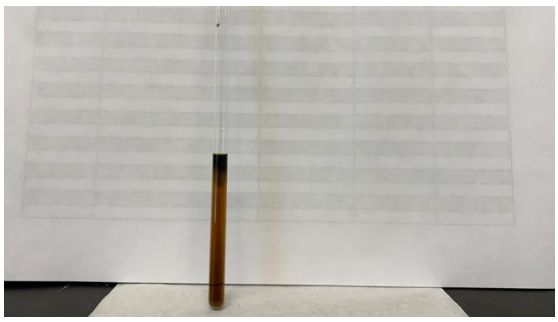

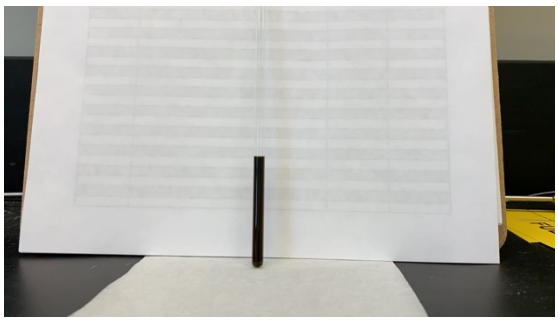

Videos S1. *Left*- Cyclic transformation over time for the oxygenation reaction of **1** with 2HAP-H (20 eq), Et_3N (2eq.) in CD_3OD with excess O_2. Darker color ensues as O_2 diffuses into the solvent. *Right*- Gradual presumed consumption of O_2 and return to starting point on the proposed catalytic reactivity of **1**.

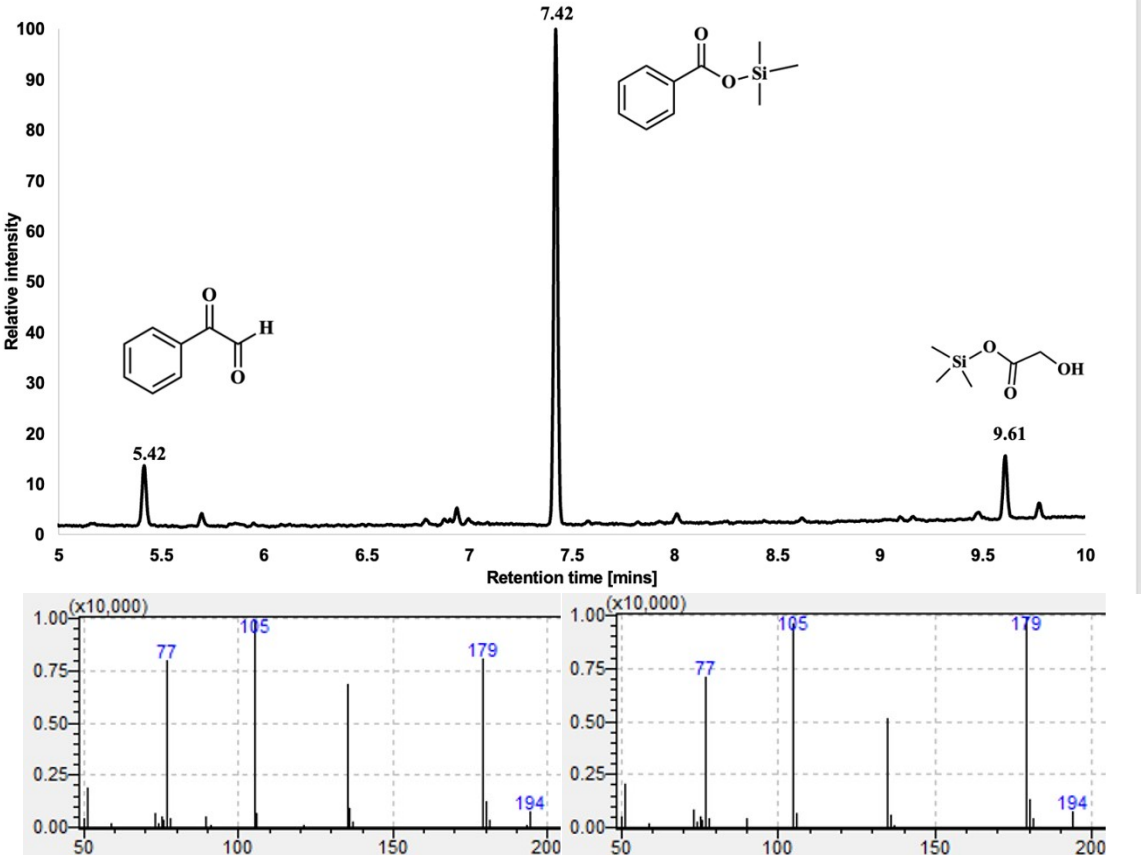

Figure S17. GC-MS of the product mixture resulting from the reaction of **1** with O_2 in the presence of 2HAP and Et_3N after aqueous acidic workup. Bottom: left: MS is the target product from the MS database, and right is the resulting product. The additional peaks at 5.42 min retention time is phenylglyoxal which is the presumed preliminary oxidation product of the substrate 2HAPH, and the peak at 9.61 is glycolic acid, trimethylsilyl ester.

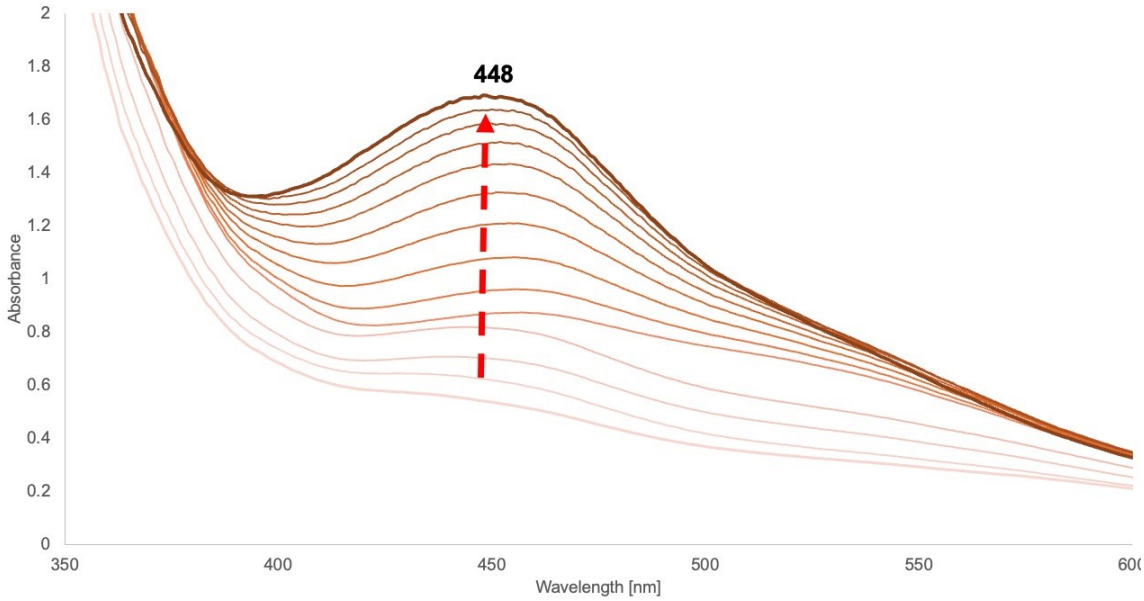

Figure S18. UV-Visible spectrum of the reaction between **1** and 1eq. of the one-electron outer sphere oxidants tris(4-bromophenyl) ammoniumyl hexachloroantimonate (magic blue) in MeOH. Growth occurs over a 1 hr period. This species is transient and decays fully in a 12 hr period.

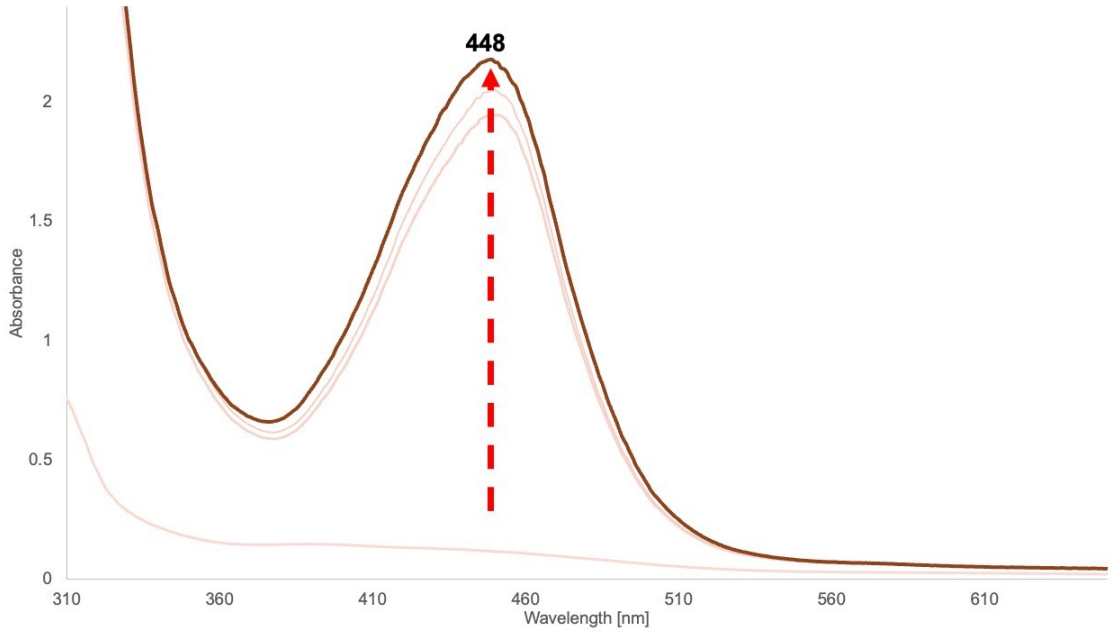

Figure S19. UV-Visible spectrum of the reaction between **1** and 1eq. of the one-electron outer sphere oxidants tris(4-bromophenyl) ammoniumyl hexachloroantimonate (magic blue) in MeCN. Growth occurs within minutes of addition. The stability of this species is of days.

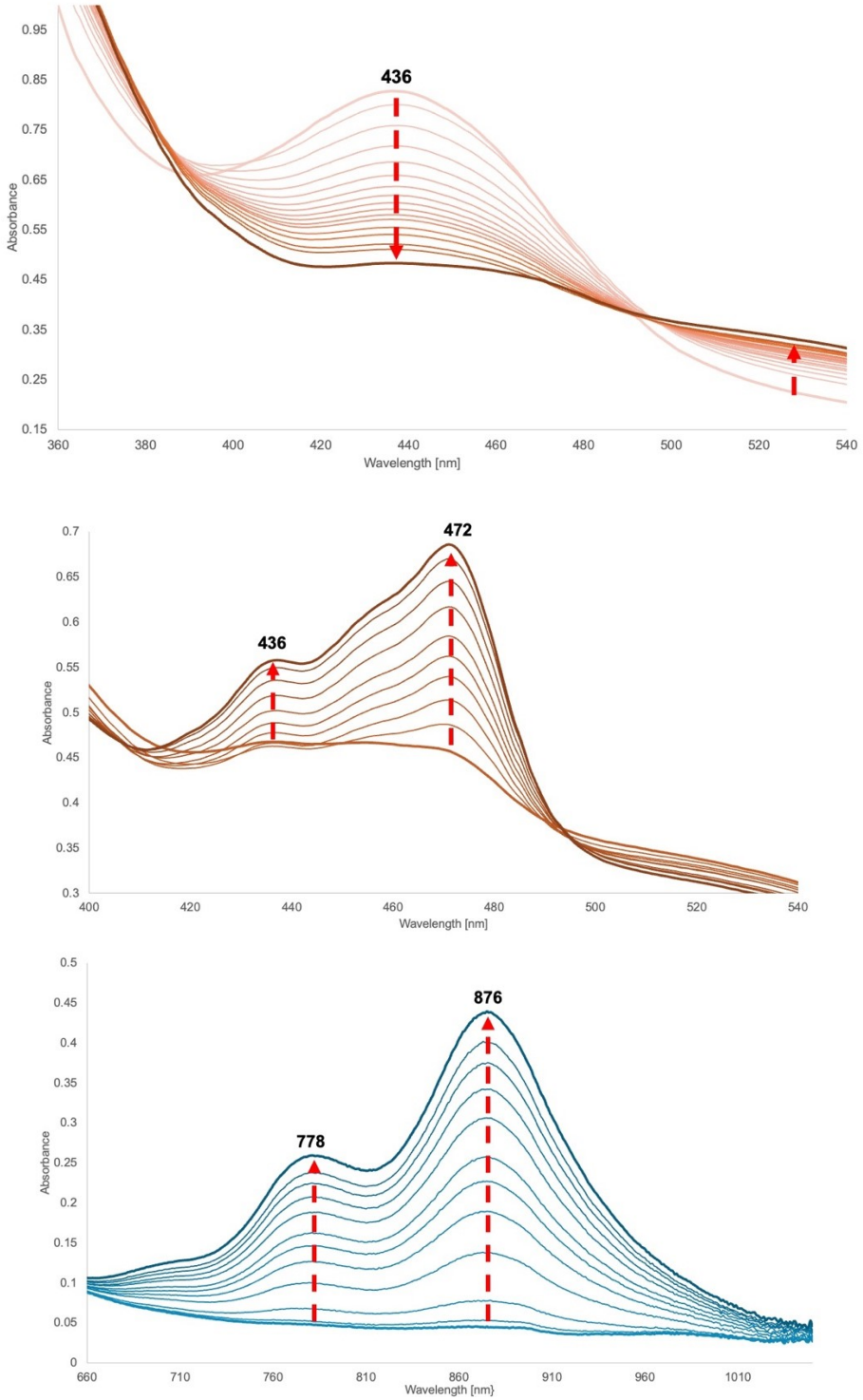

Figure S20. UV-Visible spectra of the reaction between **1** + 20 eq of 2HAP-H and 1eq. of the one-electron outer sphere oxidants tris(4-bromophenyl) ammoniumyl hexachloroantimonate (Magic Blue) in MeOH. *Top:* Immediate growth upon addition of Magic Blue. Species at 436 nm decays within 1 hr. *Middle and bottom:* Growth of a secondary species with absorbances at 436, 472, 778, and 876 nm. This occurs over a period of 1 hr. Note that this secondary species decays completely within 1 hr. after maximum absorption is obtained.

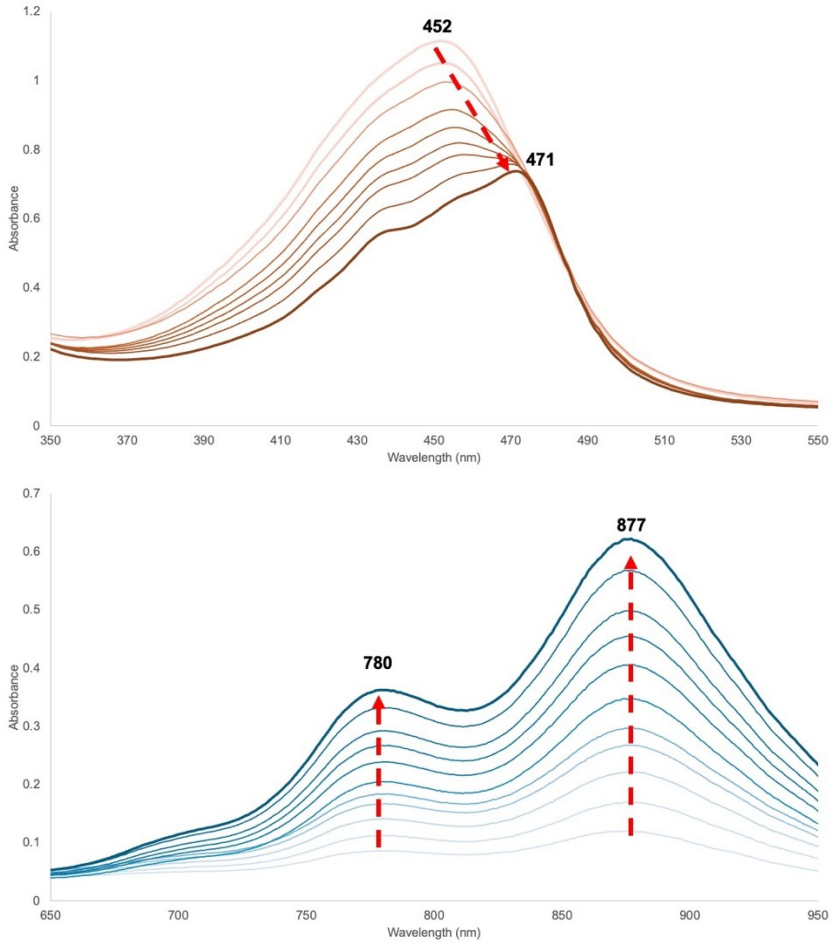

Figure S21. UV-Visible spectra of the reaction between **1** + 1eq. of the one-electron outer sphere oxidant ammonium Ce(IV) nitrate in MeCN. *Top:* Immediate growth upon addition of oxidant at 450nm. This species decays within 10 hr. to the 471 nm species. *Bottom:* Concomitant growth of a secondary species with absorbances at 436, 471, 780, and 877 nm. This occurs over a period of 10 hr. Note that this secondary species appears to be stable to decay when it was monitored over a period of 3 days.

Computational details

* For figures SX-SX (TD-DFT) all cations are doublets. All neutrals are triplets. B3LYP/def2TZVP

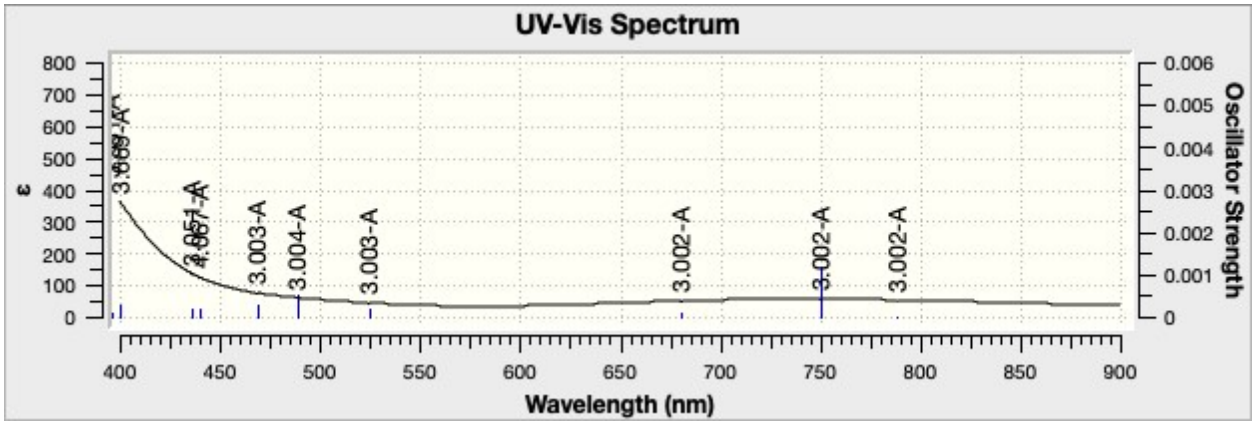

Figure S22. Neutral **1**-benzoate

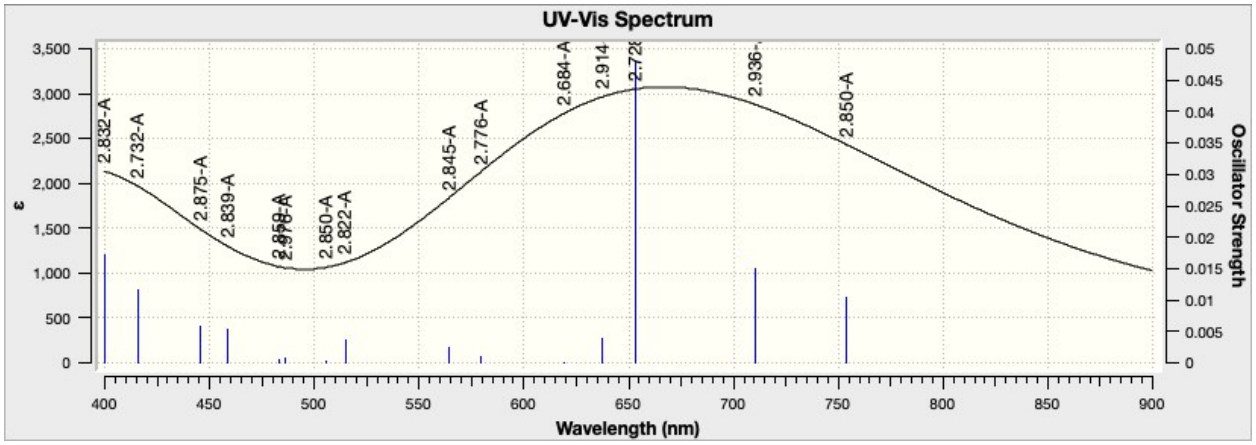

Figure S23. Cationic **1**-benzoate– intensity increases for cation, lambda-max ~ 650 nm

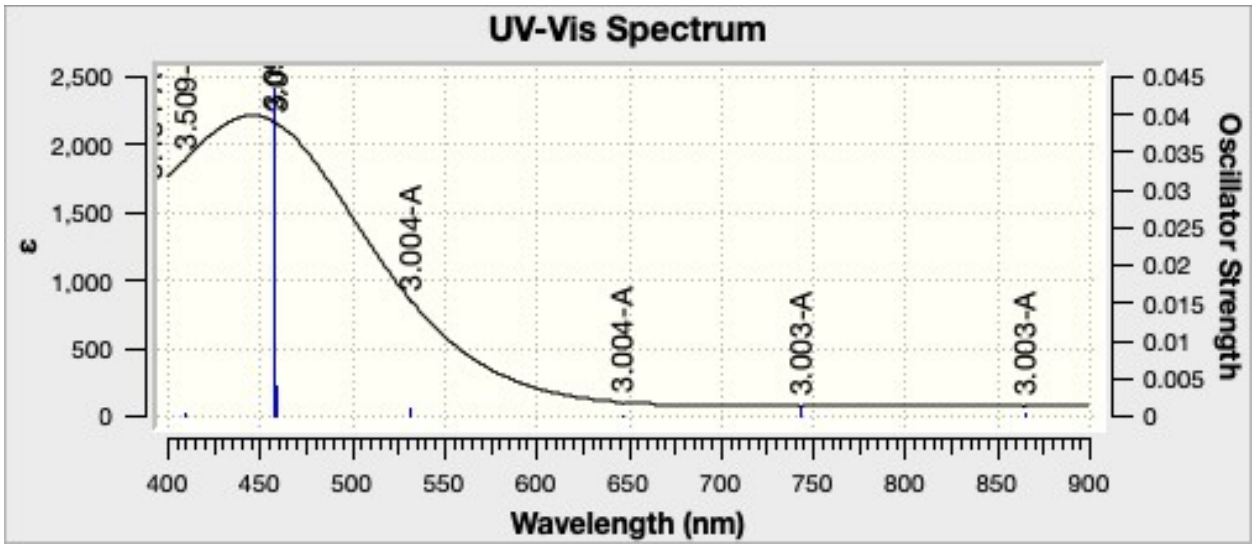

Figure S24. Neutral **1**-OTf

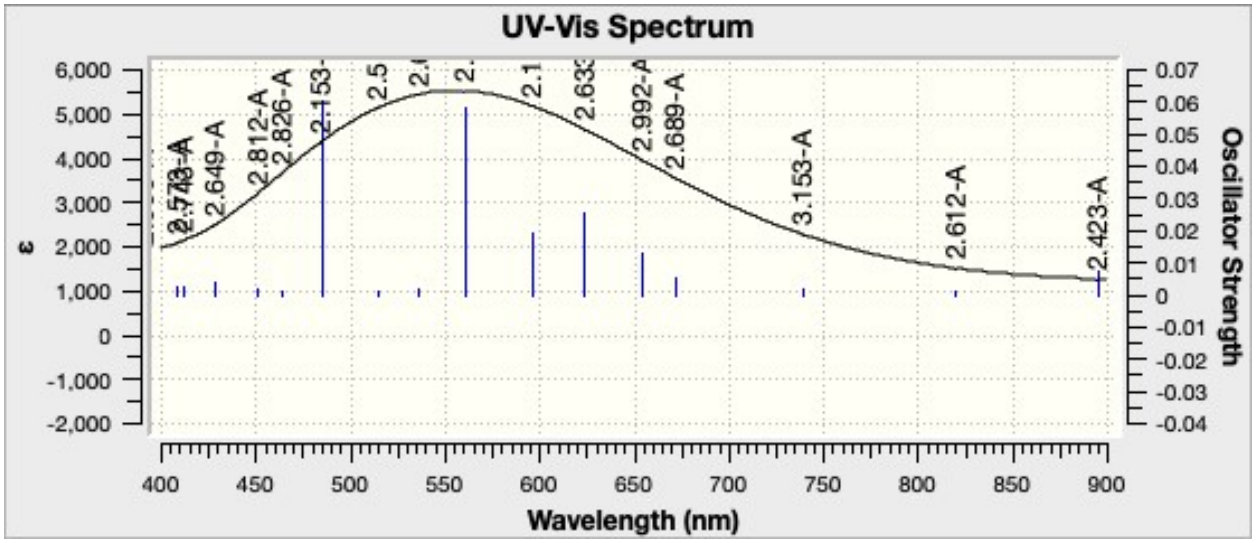

Figure S25. Cationic **1**-OTf– intensity increases for cation, shift in lambda-max from ~450 (neutral) to ~550 (cation) nm

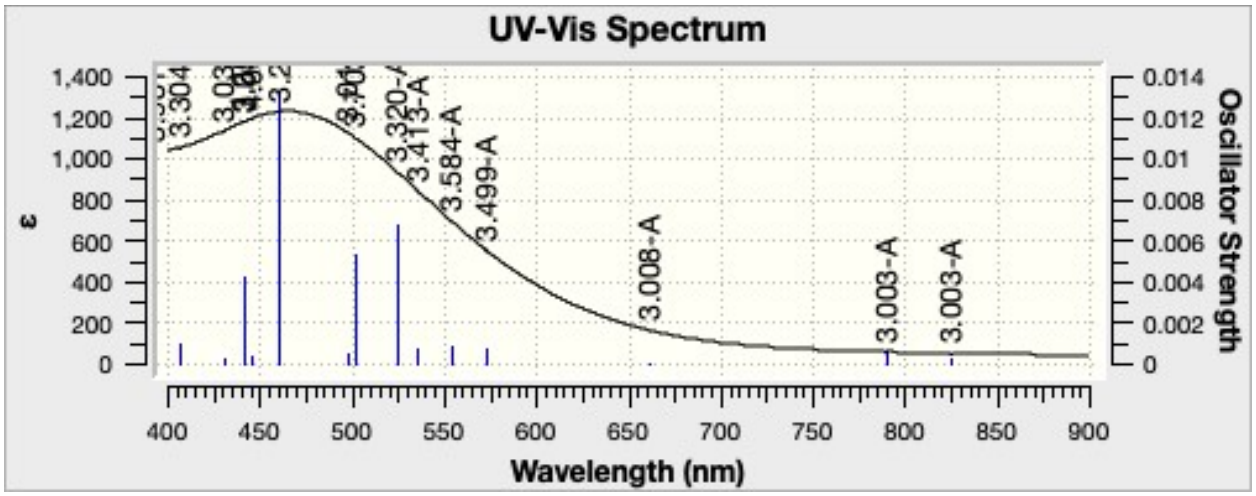

Figure S26. Neutral, **1**-2HAP

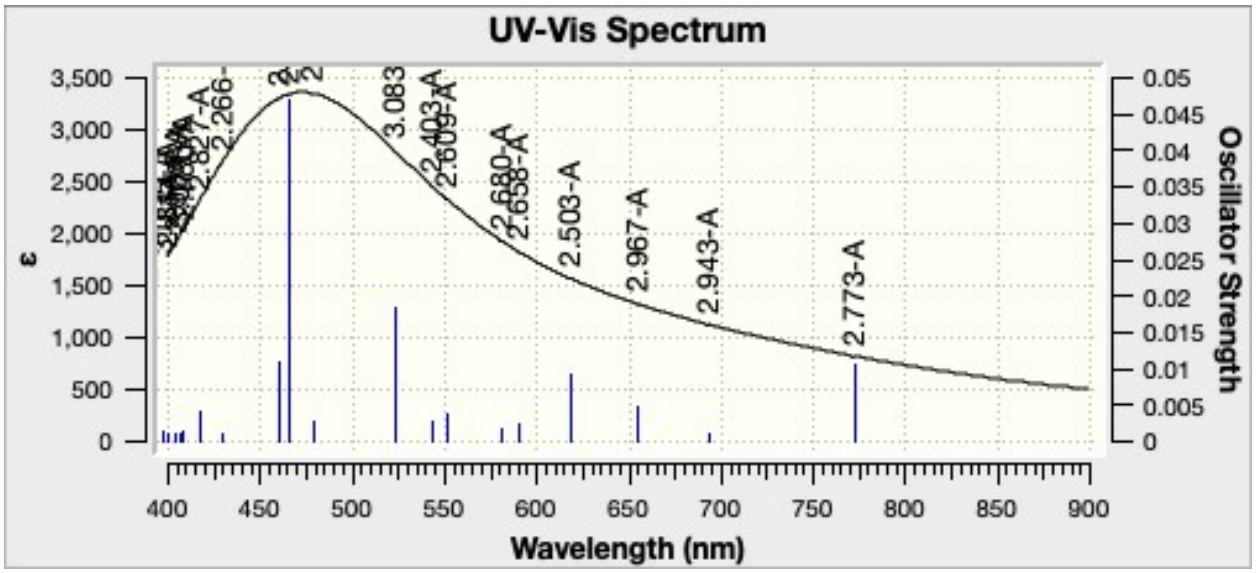

Figure S27. Cationic **1**-2HAP TD-DFT– as before, there is an increase in intensity upon oxidation of the Ni(II) complex. For the 2HAP ligand, little shift in lamda-max.

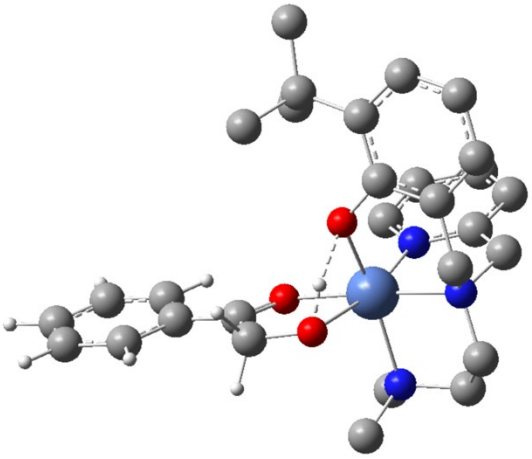

Figure S28. Core geometry of cationic, triplet **1**-2HAP-H complex. Note the H-bonding interaction between the hydroxyl proton of 2-hydroxy-acetophenone and the phenolate arm of the N_3O chelating ligand.

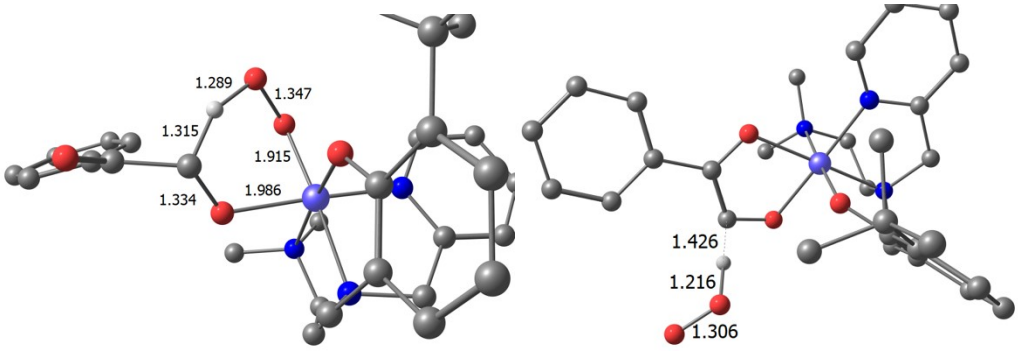

Figure S29. Comparison of inner (left) and outer (right) sphere transition states for C—H activation of alpha C_1 carbon of the 2-HAP ligand. Bond lengths in Angstrom units.

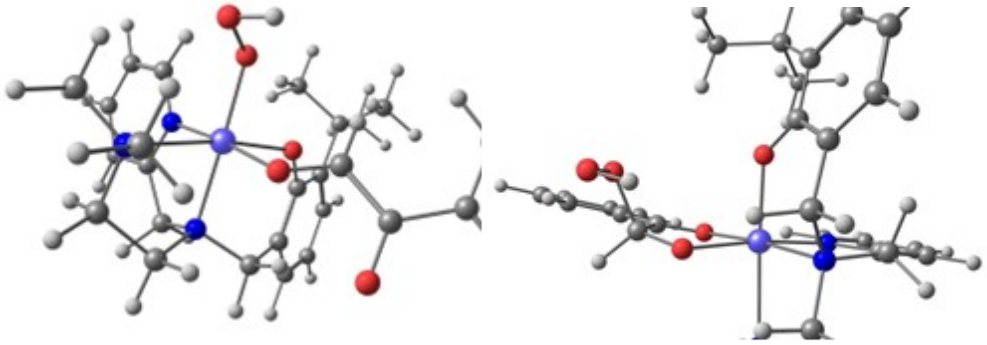

Figure S30. Comparison of Ni-OOH (left) and organic hydroperoxyl (right) intermediate complexes.

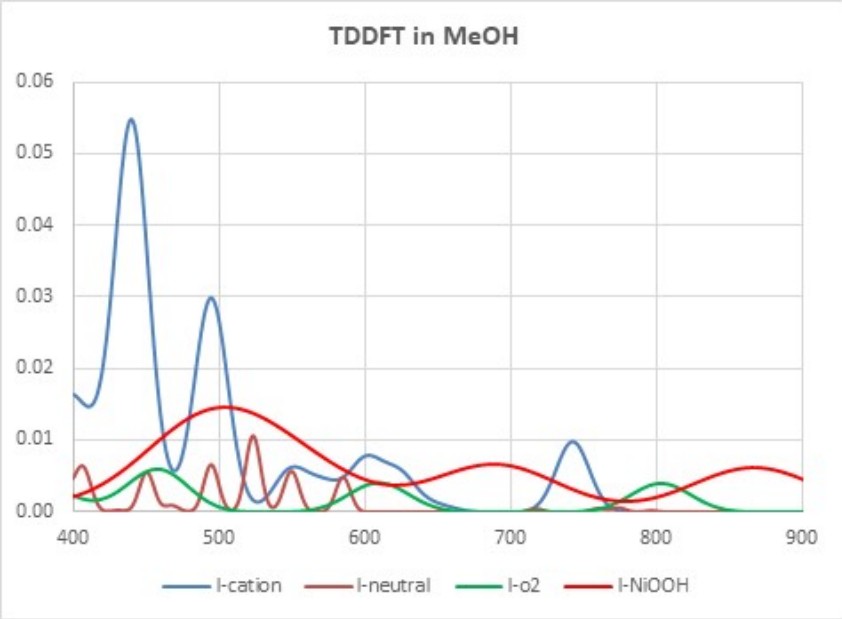

Figure S31. TD-DFT calculated UV-vis spectra for neutral **1**-2hap (orange line), its Ni(III) cation (blue line), Ni(III)-superoxide adduct (green line) and the Ni(II)-hydroperoxide (red line) generated from the latter by intramolecular C-H activation.

X-ray Data collection and refinement details

1 (CCCD identifier for compound 1: 2375944)

Crystals grew as clusters of green prisms by slow evaporation from diethyl ether into butanone. The data crystal was cut from a larger crystal and had approximate dimensions; 0.33 x 0.13 x 0.093 mm. The data were collected on a Rigaku Oxford Diffraction HyPix6000E Synergy diffractometer using a m-focus Cu Ka radiation source (λ= 1.5418Å) with collimating mirror monochromators. A total of 3240 frames of data were collected using ω-scans with a scan range of 0.5° and a counting time of 1 second per frame for frames collected with a detector offset of +/- 48.3° and 4 seconds per frame with frames collected with a detector offset of +/- 105.1°. The data were collected at 100 K using an Oxford Cryostream low temperature device. Details of crystal data, data collection and structure refinement are listed in Table 1. Data collection, unit cell refinement and data reduction were performed using Rigaku Oxford Diffraction's CrysAlisPro V 1.171.41.115a.[1] The structure was solved by direct methods using SHELXT[2] and refined by full-matrix least-squares on F^2 with anisotropic displacement parameters for the non-H atoms using SHELXL-2018/3.[3] Structure analysis was aided by use of the programs PLATON[4] and OLEX2.[5] The hydrogen atoms on the carbon atoms were calculated in ideal positions with isotropic displacement parameters set to 1.2xUeq of the attached atom (1.5xUeq for methyl hydrogen atoms).

The function, $\Sigma w(|F_o|^2 - |F_c|^2)^2$, was minimized, where $w = 1/[(\sigma(F_o))^2 + (0.0468*P)^2 + (0.763*P)]$ and $P = (|F_o|^2 + 2|F_c|^2)/3$. $R_w(F^2)$ refined to 0.0865, with R(F) equal to 0.0322 and a goodness of fit, S, = 1.04. Definitions used for calculating R(F), $R_w(F^2)$ and the goodness of fit, S, are given below.[6] The data were corrected for secondary extinction effects. The correction takes the form: $F_{corr} = kF_c/[1 + (8.0(9)x10^{-7})* F_c^2 \lambda^3/(\sin 2\theta)]^{0.25}$ where k is the overall scale factor. Neutral atom scattering factors and values used to calculate the linear absorption coefficient are from the International Tables for X-ray Crystallography (1992).[7] All figures were generated using SHELXTL/PC.[8] Tables of positional and thermal parameters, bond lengths and angles, torsion angles and figures are found elsewhere.

CCCD identifier for compound 2: 237724 Crystals grew as clusters of large, blue prisms by slow evaporation of diethyl ether into 2-butanone. The data crystal was cut from a larger crystal and had approximate dimensions; 0.28 x 0.21 x 0.15 mm. The data were collected on a Rigaku Oxford Diffraction HyPix6000E Synergy diffractometer using a m-focus Cu Ka radiation source (λ= 1.5418Å) with collimating mirror monochromators. A total of 2862 frames of data were collected using ω-scans with a scan range of 0.5° and a counting time of 0.5 seconds per frame for frames collected with a detector offset of +/- 48.3° and 2.5 seconds per frame with frames collected with a detector offset of +/- 105.1°. The data were collected at 100 K using an Oxford Cryostream low temperature device. Details of crystal data, data collection and structure refinement are listed in Table 1. Data collection, unit cell refinement and data reduction were performed using Rigaku Oxford Diffraction's CrysAlisPro V 1.171.41.115a.[1] The structure was solved by direct methods using SHELXT[2] and refined by full-matrix least-squares on F^2 with anisotropic displacement parameters for the non-H atoms using SHELXL-2018/3.[3] Structure analysis was aided by use of the programs PLATON[4] and OLEX2.[5] The hydrogen atoms on the carbon atoms were calculated in ideal positions with isotropic displacement parameters set to 1.2xUeq of the attached atom (1.5xUeq for methyl hydrogen atoms).
The function, $\Sigma w(|F_o|^2 - |F_c|^2)^2$, was minimized, where $w = 1/[(\sigma(F_o))^2 + (0.0457*P)^2 + (1.479*P)]$ and $P = (|F_o|^2 + 2|F_c|^2)/3$. $R_w(F^2)$ refined to 0.0900, with $R(F)$ equal to 0.0337 and a goodness of fit, S, = 1.03. Definitions used for calculating R(F), $R_w(F^2)$ and the goodness of fit, S, are given below.[6] The data were checked for secondary extinction effects but no correction was necessary. Neutral atom scattering factors and values used to calculate the linear absorption coefficient are from the International Tables for X-ray Crystallography (1992).[7] All figures were generated using SHELXTL/PC.[8] Tables of positional and thermal parameters, bond lengths and angles, torsion angles and figures are found elsewhere.

3 (1-Benzoic acid; CCCD identifier for compound 3: 2375818) Crystals grew as pale- yellow prisms by slow evaporation from dichloromethane. The data crystal was cut from a larger crystal and had approximate dimensions; 0.21 x 0.11 x 0.07 mm. The data were collected on a Rigaku Oxford Diffraction HyPix6000E Synergy diffractometer using a m-focus Cu Ka radiation source (λ = 1.5418Å) with collimating mirror monochromators. A total of 2244 frames of data were collected using ω-scans with a scan range of 0.5° and a counting time of 3 seconds per frame for frames collected with a detector offset of +/- 48.3° and 11 seconds per frame with frames collected with a detector offset of +/- 104.5°. The data were collected at 100 K using an Oxford Cryostream low temperature device. Details of crystal data, data collection and structure refinement are listed in Table 1. Data collection, unit cell refinement and data reduction were performed using Rigaku Oxford Diffraction's CrysAlisPro V 1.171.41.123a.[1] The structure was solved by direct methods using SHELXT[2] and refined by full-matrix least-squares on F^2 with anisotropic displacement parameters for the non-H atoms using SHELXL-2018/3.[3] Structure analysis was aided by use of the programs PLATON[4] and OLEX2.[5] The hydrogen atoms on the carbon atoms were calculated in ideal positions with isotropic displacement parameters set to 1.2xUeq of the attached atom (1.5xUeq for methyl hydrogen atoms).

There are two Ni complexes in the asymmetric unit that are related by a pseudo inversion center near 3/8, ¾, ¾. The complexes deviate from centrosymmetry due to the coordination of the triflate ions. Triflate ions are disordered to a different extent. The predominant triflate ion bound to Ni2 has an occupancy factor of 87%, while the predominant triflate ion on Ni2 has an occupancy factor of 69%. The predominant triflate ions break the inversion symmetry.

The function, $\Sigma w(|F_o|^2 - |F_c|^2)^2$, was minimized, where $w = 1/[(\sigma(F_o))^2 + (0.107*P)^2 + (1.9703*P)]$ and $P = (|F_o|^2 + 2|F_c|^2)/3$. $R_w(F^2)$ refined to 0.148, with R(F) equal to 0.0520 and a goodness of fit, S, = 1.03. Definitions used for calculating R(F), $R_w(F^2)$ and the goodness of fit, S, are given below.[6] The data were checked for secondary extinction effects, but no correction was necessary. Neutral atom scattering factors and values used to calculate the linear absorption coefficient are from the International Tables for X-ray Crystallography (1992).[7] All figures were generated using SHELXTL/PC.[8] Tables of positional and thermal parameters, bond lengths and angles, torsion angles and figures are found elsewhere.

Table S1. Crystal data and refinement parameters for **1**, **2, 3**

	1	**2**	**3**
Empirical formula	C22 H30 F3 N3 Ni O4 S	C26 H37 N3 Ni O3	C30 H37 Cl2 F3 N3 Ni O6 S
Formula weight	548.26	498.29	**754.29**
Temperature	99.98(19) K	100.0(5) K	100.0(6) K
Wavelength	1.54184 Å	1.54184 Å	1.54184 Å
Crystal system	triclinic	monoclinic	**monoclinic**
Space group	P -1	P 1 21/c 1	P 1 c 1
Unit cell dimensions	a = 9.39775(11) Å a= 93.7250(8)°. b = 10.41762(10) Å c = 13.43710(11) Å g = 99.7261(9)°.	a = 11.61580(14) Å a= 90°. b = 15.48907(15) Å b= 106.8157(12)°. c = 14.59532(16) Å g = 90°.	a = 17.2655(3) Å a= 90° b = 11.9834(2) Å b= 108.252(2)°. c = 16.9887(3) Å g = 90°.
Volume	1207.28(2) $Å^3$	2513.67(5) $Å^3$	3338.11(11) $Å^3$
Z	**2**	**4**	**4**
Density (calculated)	1.508 Mg/m^3	1.317 Mg/m^3	1.501 Mg/m^3
Absorption coefficient	2.478 mm^{-1}	1.361 mm^{-1}	3.447 mm^{-1}
F(000)	572	**1064**	1564
Crystal size	0.33 x 0.13 x 0.093 mm^3	0.28 x 0.21 x 0.15 mm^3	0.216 x 0.114 x 0.07 mm^3
Theta range for data collection	3.533 to 76.413°.	3.976 to 76.710°.	2.695 to 76.269°.
Index ranges	-11<=h<=11, -13<=k<=13, -16<=l<=16	-14<=h<=14, -10<=k<=19, -18<=l<=18	-21<=h<=21, -11<=k<=14, -21<=l<=21
Reflections collected	13150	24090	**25771**
Independent reflections	4821 [R(int) = 0.0165]	5168 [R(int) =	8632 [R(int) = 0.0277]

		0.0283]	
Completeness to theta = 67.684°	98.9 %	100.0 %	99.0 %
Refinement method	Full-matrix least-squares on F^2	Full-matrix least-squares on F^2	Full-matrix least-squares on F^2
Data / restraints / parameters	4821 / 337 / 372	5168 / 0 / 305	8632 / 669 / 932
Goodness-of-fit on F2	1.046	1.033	1.050
Final R indices [I>2sigma(I)]	R1 = 0.0322, wR2 = 0.0861	R1 = 0.0337, wR2 = 0.0893	R1 = 0.0520, wR2 = 0.1460
R indices (all data)	R1 = 0.0327, wR2 = 0.0865	R1 = 0.0345, wR2 = 0.0900	R1 = 0.0533, wR2 = 0.1477
Extinction coefficient	$8.0(19)x10^{-7}$	n/a	n/a
Largest diff. peak and hole	0.417 and -0.347 e.$Å^{-3}$	0.420 and -0.397 e.$Å^{-3}$	0.682 and -0.879 e.$Å^{-3}$

Crystallographic References

1) CrysAlisPro. Rigaku Oxford Diffraction, HyPix6000E System, CrysAlisPro Software System, 1.171.41.115a.

2) SHELXT. (2015). G. M. Sheldrick. A program for crystal structure solution. Acta Cryst. A71, 3-8.

3) Sheldrick, G. M. (2015). SHELXL-2018/3. Program for the Refinement of Crystal Structures. Acta Cryst., C71, 9-18.

4) Spek, A. L. (2009). PLATON, A Multipurpose Crystallographic Tool. Utrecht University, The Netherlands. Acta Cryst. D65, 148-155.

5) OLEX2. Dolomanov, O. V., Bourhis, L. J., Gildea, R. J., Howard, J. A. K. and Puschmann, H. A Complete Structure Solution, Refinement and Analysis Program. J. Appl. Cryst. 42, 339-341.

6) $R_W(F^2) = \{\Sigma w(|F_o|^2 - |F_c|^2)^2/\Sigma w(|F_o|)^4\}^{1/2}$ where w is the weight given each reflection.
$R(F) = \Sigma(|F_o| - |F_c|)/\Sigma|F_o|\}$ for reflections with $F_o > 4(\sigma(F_o))$.
$S = [\Sigma w(|F_o|^2 - |F_c|^2)^2/(n - p)]^{1/2}$, where n is the number of reflections and p is the number of refined parameters.

7) International Tables for X-ray Crystallography (1992). Vol. C, Tables 4.2.6.8 and 6.1.1.4, A. J. C. Wilson, editor, Boston: Kluwer Academic Press.

8) Sheldrick, G. M. (1994). SHELXTL/PC (Version 5.03). Siemens Analytical X-ray Instruments, Inc., Madison, Wisconsin, USA.